# Tunable THz plasmon resonances in InGaAs/InP HEMT

R. E. Peale[*a], H. Saxena[a], W. R. Buchwald[b], G. C. Dyer[c], S. J. Allen, Jr.[c]
[a]University of Central Florida, Department of Physics, Orlando, FL USA 32765; [b] Air Force Research Laboratory, Hanscom AFB MA USA 01731; [c]University of California Santa Barbara, Department of Physics, Santa Barbara CA USA 93106

## ABSTRACT

Voltage-tunable plasmon resonances in a InGaAs/InP high electron mobility transistor (HEMT) are reported. The gate contact consisted of a 0.5 micron period metal grating formed by electron-beam lithography. Narrow-band resonant absorption of THz radiation was observed in transmission in the range 10 – 50 $cm^{-1}$. The resonance frequency red-shifts with increasing negative gate bias as expected. Photo-response to a tunable far-IR laser is reported. The device may have application in high-frame-rate THz array detectors for spectral imaging with real-time chemical analysis.

**Keywords:** Terahertz, two dimensional electron gas, plasmon, detector, HEMT

## 1. INTRODUCTION

Resonant absorption of terahertz radiation by plasma oscillations in two dimensional electron gases (2degs) [1, 2] can affect source-drain conductance, a photo-response that is the basis for proposed frequency-agile terahertz (THz) detectors [3]. Gate bias control of sheet charge density $n_s$ allows continuous tuning of the resonance over a wide range. A gate in the form of a metallic transmission grating couples externally incident THz radiation to plasmons in the 2DEG, while the grating period $a$ defines the plasmon wavevector $g_p = 2\pi p/a$, with $p$ the integer resonance order. The resonance frequency ω is determined by the dispersion relation [1]

$$\omega = \sqrt{\left(\frac{n_s e^2}{m^*}\right)\left(\frac{g_p}{\varepsilon_o\left(\varepsilon_b + \varepsilon_t Coth(g_p d)\right)}\right)} \quad , \tag{1}$$

where $\varepsilon_b$ is the relative permittivity of the material below the 2deg, $\varepsilon_t$ that above, $\varepsilon_0$ the permittivity of free space, m* the effective electron mass, $e$ the charge, and $d$ the gate-2deg separation. High fundamental frequency requires small $a$, high $n_s$, and small $m^*$. A variety of materials systems such as GaAs/AlGaAs [3], InGaP/InGaAs/GaAs [4], GaN/AlGaN [2, 5] and Si [1] have been explored, all except the last forming high electron mobility transistors (HEMTs) while the Si system was a metal-oxide-semiconductor field-effect transistor (MOSFET). This paper reports THz absorption resonances in a HEMT fabricated in the InGaAs/InP system and first measurements of an electrical photoresponse. This materials system features high $n_s$ and low $m^*$, so that this system has potential to realize fundamental plasmon resonances at wavelengths shorter than those previously obtainable in Si [1] or GaAs [3].

## 2. EXPERIMENT

The MBE grown structure of the commercial 100 mm diameter HEMT wafer (IQE) is shown in Fig. 1 (left). The 25 nm thick cap was removed before gate metallization using a 27:1 selective etch, putting the 2DEG in the InGaAs channel at $d$ = 44.5 nm below the gate. Fig. 1 (center) presents a scanning electron micrograph of the device metallization, which is that of a typical HEMT except for the large gate with length $L$ = 195 μm and width $W$ = 250 μm. Metallization of the entire 3.5 mm x 3.5 mm die was designed to allow transmittance only through the gated area. An inter-level dielectric of B-staged Bisbenzocyclobutane-based polymer (BCB) allowed overlapping metal layers to block light transmission outside the gate while maintaining electrical isolation. With the addition of a metal layer around the entire device, the gate acts as an aperture for a detector placed behind the device during spectroscopic characterization. Fabrication was undertaken using standard optical contact lithography and a combination of wet chemical etching for the semiconductor and dry etching for the BCB. No BCB was left over the gate opening in order to maximize optical throughput. After

removal of the InGaAs cap in the gate region, the gate/grating was formed in two steps. A thin Ti layer (7.5 nm) was first evaporated over the entire patterned gate area. This thickness is sufficiently less than the THz skin depth to allow for transmittance measurements. It was made continuous in order to achieve uniform gate control of the 2deg sheet charge. The gate/grating was then fabricated using e-beam lithography. After spin coating with positive tone PMMA, 30 keV electrons patterned grating stripes with period 0.5 μm. A metal stack of 150 Å/1000 Å Ti/Au was then evaporated and lifted, completing the fabrication of the grating. The Fig. 1 (center) inset presents a higher magnification image of the grating. Here the metal stripes are thinner than the gaps between them, and this sample was used for FTIR transmission studies. For photoresponse studies, a grating with the inverse duty cycle (wide metal, thin gaps, Fig. 1 right) was used, due to the stronger coupling to plasmons expected from calculations for such structures.

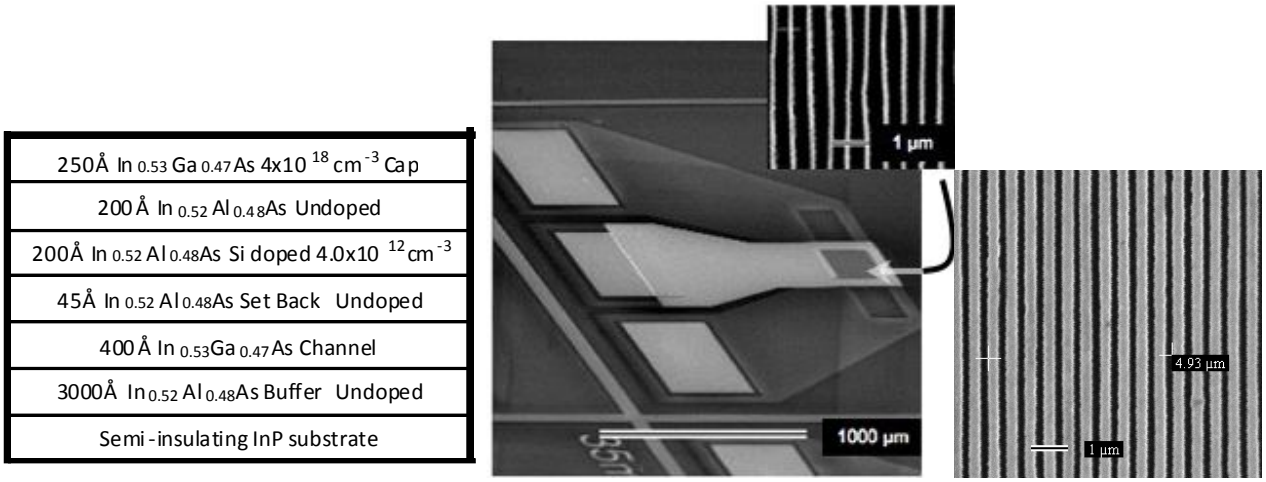


Fig. 1. (left). MBE grown epilayer structure used for fabrication of the HEMT. (center) SEM micrograph of device. The large pads on the left of the image are for wire bonding. The inset is a blow-up of the gate region, showing the grating metallization for the low duty grating used in transmittance experiments. (right) Micrograph of the high-duty grating used for the device used in photoresponse experiments.

Far-infrared transmission spectroscopy was performed using a Fourier spectrometer as described in [6]. The UCSB mm-wave free electron laser (FEL) was used to search for resonant photo-response in the device, which was mounted in a temperature-controlled closed-cycle cooler. The FEL pulse repetition rate was ~ 1 Hz and pulse duration ~1 μs. Pulse energy was measured and recorded for every laser shot. The polarization was horizontal but could be rotated to vertical using wire-grid polarizers. The device was oriented so that the grating stripes were vertical. Crossed polarizers were used to determine the FEL power dependence of the observed photo-response. The gate was biased using a battery and potentiometer in the range -0.5 to 0.3 V. Two different schemes were used to apply the source-drain bias. The first biasing scheme, shown in Figure 2 (a), used a current supply to provide constant source-drain current $I_{SD}$ through the device with the drain grounded, while the voltage across the device $V_{SD}$ was monitored on an AC coupled oscilloscope as a function of gate bias $V_{GD}$. In the second scheme, (Figure 2(b)), the HEMT was biased with a constant 0.25 mV at the source and a load resistor, $R_L$, of 10 kΩ from drain to ground. The voltage drop, $V_L$, across the load was monitored on an oscilloscope synchronous with the FEL pulses. As expected, the steady state dark value of $V_{SD}$ (= 0.25mV – $V_L$), does change as the gate voltage sweeps, indicating proper gate control. However, because of the small source bias condition, the change in $V_{SD}$ from $V_G = 0$ to pinch-off remains less than 10 mV. Data with a small $R_L$ (100 Ω) and with large $V_S = 0.5$ V was also collected. In addition, a shunt capacitor of C = 100 nF connected from source to ground was experimented with in order make the circuit time constant longer relative to the FEL pulse width. This assures that the power supply can adequately adjust to fix the voltage on the time scale defined by $R_L C$ . As expected, with the shunt capacitor, there was less noise.

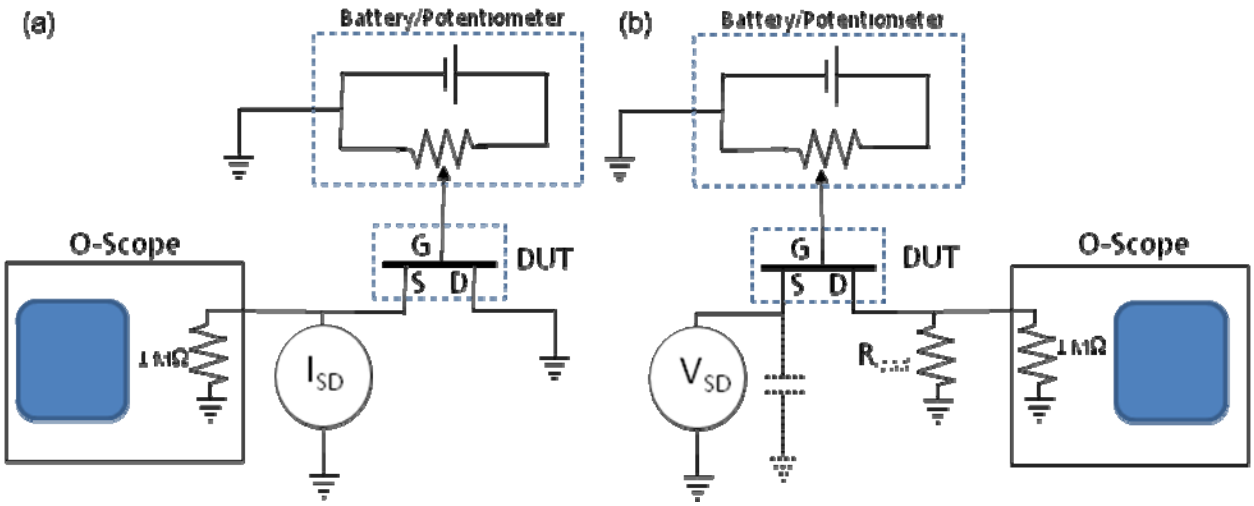


Fig. 2. (a). Constant current scheme used for device biasing in this work. And (b), constant voltage scheme

## 3. RESULTS

FTIR transmission spectra reveal resonant absorption, as presented in Fig. 3 (left). The absorption is manifested as an extinction of Fabry-Perot resonances from the substrate. (Negative signal and inverted absorption features are results of phase errors due to the low throughput of the sub-wavelength gate aperture.) Fig. 3 (right) presents a plot of the observed center frequencies in the range 10-50 $cm^{-1}$ as a function of gate bias $V_G$ with source and drain grounded. The shift of the resonances with gate bias is qualitatively in agreement with theoretical expectations, although the absolute frequency values and their ratios disagree somewhat from the values expected from Eq. 1. Experimentally we find that the lowest resonance shifts from a frequency of ~25 $cm^{-1}$ at zero gate bias to a frequency of ~15 $cm^{-1}$ near pinch-off.

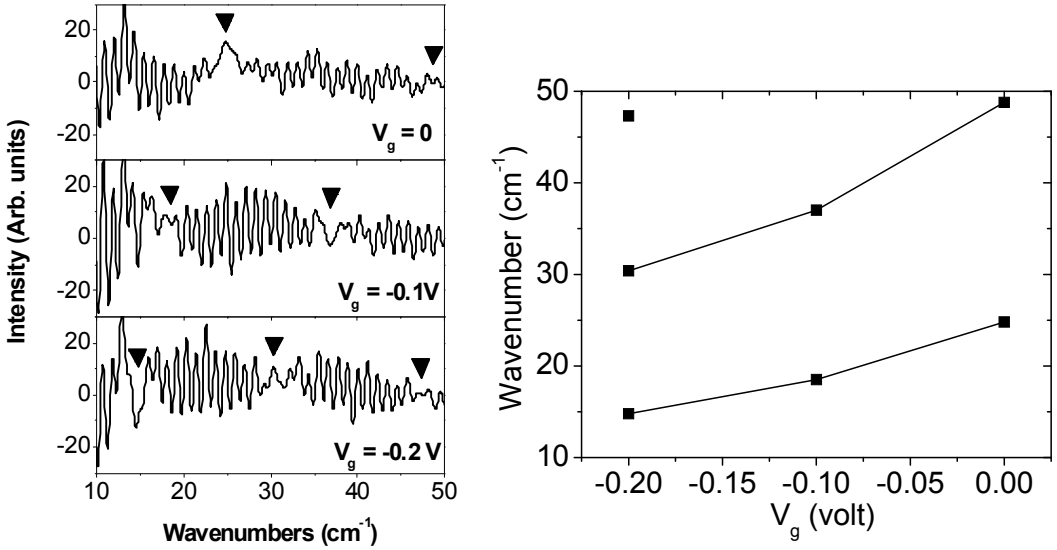


Fig. 3. (left) Transmittance spectrum of grating gated HEMT. (right) Measured resonance wavenumber as a function of gate bias. Sample temperature is ~ 20 K.

In photoresponse experiments, using the constant current biasing scheme with $I_{SD}$ = 0, a negative photovoltage of order 10 mV was observed between source and drain coincident with the laser pulse. The photoresponse changed sign and was much smaller in magnitude when the polarization was rotated to the vertical using a pair of polarizers sequentially at 45

and 90 degrees with respect to the horizontal. This gave a THz electric field polarized parallel to the grating stripes. During this observation the intensity on the sample was maintained constant.

The $\Delta V_{SD}$ was found to have a sub-linear dependence on laser pulse energy P, as shown in Fig. 4. At low powers, the data go as the square root of the pulse energy, but at higher powers the data approach a straight line. Normalization of the measured $\Delta V_{SD}$ by P fails to correct adequately for shot-to-shot energy variations, such that significant artifacts appear in data so normalized. To reduce such artifacts, the measured $\Delta V_{SD}$ were normalized instead to a quadratic function $AP + BP^2$ of pulse energy P. The coefficients A and B were determined from a fit to $\Delta V_{SD}$ data measured in the unbiased device as a function of P. Fig. 4 presents examples of these measurements. Independent data taken at the same wavenumber need not coincide: Pulse energy at the sample for the same beam intensity changes with the alignment and focus conditions. Since these conditions were adjusted several times during the several days of experimentation, it is impossible to make any conclusion from Fig. 4 concerning the wavelength dependence of the photoresponse. Different fitting coefficients were determined for each curve and used to correct data taken under the same conditions. Experimental $\Delta V_{SD}$ points normalized in this way have positive sign.

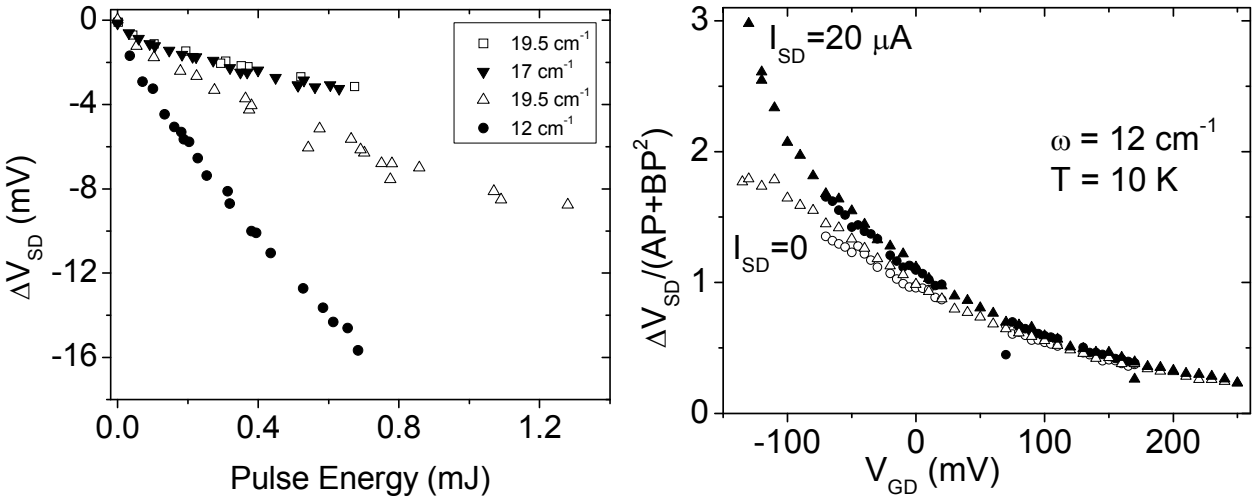


Fig. 4. Zero-bias photo response as a function of laser pulse energy at three different THz frequencies.

Fig. 5. Device photoresponse with and without current bias as a function of gate bias at a frequency of 12 $cm^{-1}$.

With $I_{SD}$ = 20 μA applied, the magnitude of the photoresponse increased, indicating a THz induced increase in channel resistance. Near pinch off, this increase (which we refer to as the photo*conductive* component in the total signal) exceeded the zero-bias photovoltage. Far from pinch off, the increase was negligible. Fig. 5 presents the normalized $\Delta V_{SD}$ vs. gate bias $V_{GD}$ with and without source bias $I_{SD}$ for a FEL frequency of 12 $cm^{-1}$, where according to Fig. 2 no resonance is anticipated. Apart from some non-repeatable weak bumps and outliers, nothing like a resonance is observed in either curve.

Figure 6 presents photoresponse data at a frequency of 17 $cm^{-1}$. According to Fig. 3, a resonance might be expected at a gate voltage of about -150 mV. However, due to the constant $I_{SD}$ biasing and a reluctance to allow $V_{SD}$ to exceed 0.5 V, the value $V_{GD}$ = -150 mV was unattainable. A strong feature observed once near a gate bias of -75 mV was unrepeatable.

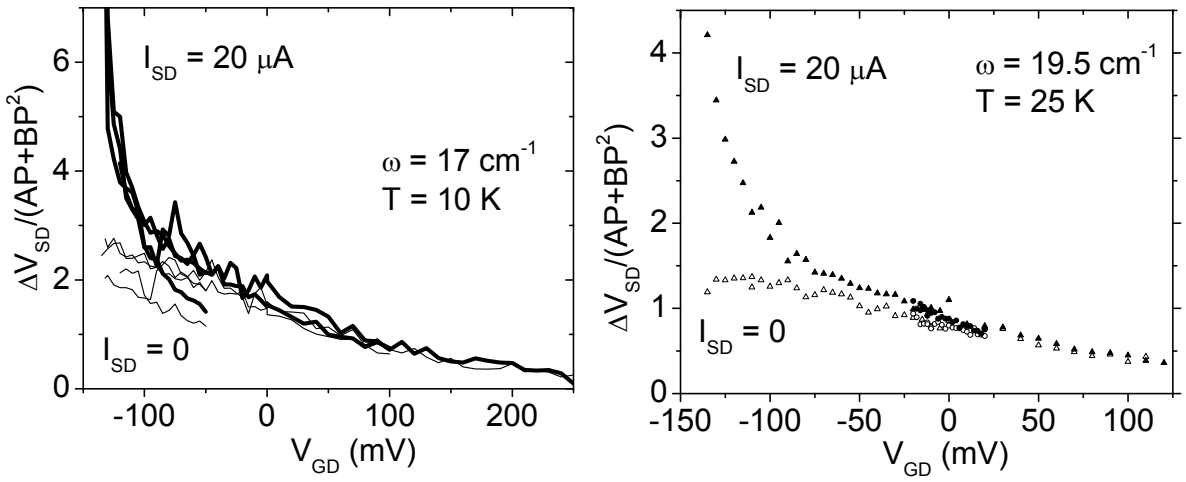


Fig. 6. Device photoresponse with (heavy lines) and without (light lines) current bias as a function of gate bias at a frequency of 17 $cm^{-1}$.

Fig. 7. Device photoresponse with (solid symbols) and without (open symbols) current bias as a function of gate bias at a frequency of 19.5 $cm^{-1}$.

Figure 7 presents photoresponse data at a frequency of 19.5 $cm^{-1}$. According to Fig. 2, a resonance might appear at a gate voltage of about -80 mV, which is in range of the experiment for constant $I_{SD}$ = 20 μA biasing. There may be a bump near this gate voltage, but it is very weak and could easily be noise.

Results for constant voltage bias, schematically shown in Figure 2 (b), are presented in Fig. 8 at frequency 17 $cm^{-1}$ for large load resistance and small bias, and also for small load and large bias. With this method of biasing, the photoresponse is positive. Here the photoresponse was best fit to a pulse energy dependence of $A\sqrt{P} + BP$, and hence the data is normalized by this function. The photo response is one order larger in the large load case. As mentioned above, the fundamental plasmon resonance occurs near $V_G$ = -150 mV at this wavenumber (Fig. 2), but no resonance effect on transport is detected at this gate bias in Fig. 8.

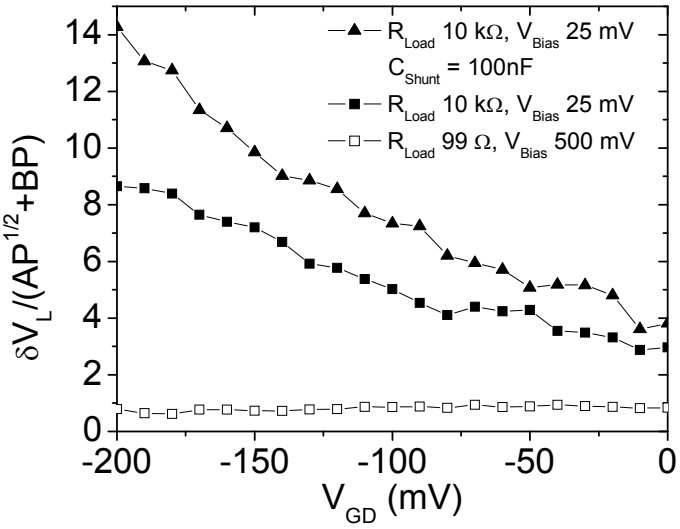


Fig. 8. Device photoresponse with constant voltage bias $V_S$ as a function of gate bias $V_G$ at frequency 17 $cm^{-1}$ for different bias $V_S$, different load resistance $R_L$, and in one case with a shunt capacitor.

## 4. SUMMARY.

In summary, two-dimensional plasma oscillations in the electron gas of an InGaAs/InP HEMT device have been clearly seen in far-IR transmission spectra. An initial search for an effect of such resonances on transport, using a mm-wave free electron laser, was less conclusive. We suggest that the effect may be masked or altered by the large non-resonant non-linear response to the incident THz radiation and by noise or artifacts induced by pulse energy-variations of the free electron laser. The metallization pattern that was designed with transmission measurements in mind may enhance that response by acting as an antenna.

## REFERENCES

[1] Allen, S. J., Tsui, D. C., Logan, R. A., "Observation of the two-dimensional plasmon in silicon inversion layers," Phys. Rev. Lett. 38, 980-983 (1977).

[2] Knap, W., Deng, Y., Rumyantsev, S., and Shur, M. S., "Resonant detection of subterahertz and terahertz radiation by plasma waves in submicron field-effect transistors ," Appl. Phys. Lett. 81, 4637-4639 (2002).

[3] Peralta, X. G., Allen, S. J., Wanke, M. C., Harff, N. E., Simmons, J. A., Lilly, M. P., Reno, J. L., Burke, P. J. and Eisenstein, J. P., "Terahertz photoconductivity and plasmon modes in double-quantum-well field-effect transistors," Appl. Phys. Lett. 81, 1627-1629 (2002).

[4] Otsuji, T., Hanabe, M., and Ogawara, O., "Terahertz plasma wave resonance of two-dimensional electrons in InGaP/InGaAs/GaAs high-electron-mobility transistors," Appl. Phys. Lett. 85, 2119-2121 (2004).

[5] Knap, W., Kachorovskii, V., Deng, Y., Rumyantsev, S., Lü, J.-Q., Gaska, R., Shur, M. S., Simin, G., Hu, X., Asif Khan, M., Saylor, C. A., and Brunel, L. C. "Nonresonant detection of terahertz radiation in field effect transistors," Appl. Phys. Lett. 91, 9346-9354 (2002).

[6] Saxena, H., Peale, R. E., and Buchwald, W. R., "Tunable two-dimensional plasmon resonances in an InGaAs/InP high electron-mobility transistor," J. Appl. Phys. (2009), accepted.

[7] Buchwald, W. R., Saxena, H., Peale, R. E., "Tunable far-IR detectors/filters based on plasmons in two-dimensional electron gases in InGaAs/InP heterostructures," Proc. SPIE 6678-32 (2007).